Data preparation for the determination of the far-field diffraction pattern of satellite's retroreflectors by Satellite Laser Ranging

Stefanie Häusler
Deggendorf Institute of Technology
Deggendorf, Germany
Email: stefanie.haeusler@stud.th-deg.de

Johann Josef Eckl
Federal Agency for Cartography and Geodesy
Wettzell, Germany
Email: johann.eckl@bkg.bund.de

***Abstract*—State-of-the-art Satellite Laser Ranging (SLR) systems provide a ranging accuracy at a level of a few millimeters. Nonetheless, tasks like the determination of the scale GM with the universal gravitational constant G and the mass of the earth M or upcoming challenges like Laser Time Transfer require an even higher accuracy. Currently, uncertainties resulting during the transmission of the laser beam through the turbulent atmosphere are suspect to introduce systematic errors. The atmosphere leads to hardly predictable time delays and eddies cause fluctuations of the signal strength as well as a displacement and a spread of the beam. There is evidence that the far-field diffraction pattern (FFDP) of the retroreflectors on board of the satellites is a key to improve the situation. As the Geodetic Observatory Wettzell is equipped with two SLR systems, the Satellite Observing System Wettzell (SOSW) and the Wettzell Laser Ranging System (WLRS), which are located close to each other, the determination of the FFDP of low earth orbit satellites is possible. In order to carry out an organized analysis of this experiment, a database was set up. Apart from the passage information: azimuth, elevation and range, the database contains the following criteria: astronomical seeing predictions, orientation of the retroreflector with respect to the SOSW and the velocity aberration of the satellites. Both of the latter have to be calculated for the various constellations. The structure of the data base and the calculation of the criteria are described to ensure a high transparency of the experiment.**

***Keywords*—Satellite Laser Ranging, far-field diffraction pattern, retroreflector, optical response**

GLOSSARY OF TERMS

COM	center-of-mass
FFDP	far-field diffraction pattern
SLR	Satellite Laser Ranging
SOD	seconds of the day
SOSW	Satellite Observing System Wettzell
WLRS	Wettzell Laser Ranging System

I. INTRODUCTION

Modern Satellite Laser Ranging (SLR) systems provide millimeter precision. An even higher precision is required. The main task of SLR, which is the determination of the scale GM with the universal gravitational constant G and the mass of the earth M, would benefit from such an approach. Furthermore, upcoming new tasks like Laser Time Transfer will also need a higher precision. Since the issues caused by the timing accuracy of the hardware are invented at an even high level, the remaining limiting uncertainties are the atmosphere and the satellite signature effect. The atmosphere causes fluctuations of the return signal strength and a time delay through atmospheric turbulence and temperature, humidity and pressure differences. Moreover, the satellite signature effect is caused by the multiple onboard reflectors which spread the optical pulse signal. It is assumed that both affect the target response function which has an impact on the center-of-mass (COM) correction of the satellite. The COM correction is associated with the displacement of the retroreflector arrays from the COM of the satellite. Therefore, it needs to be added to the measured distance in order to calculate the orbit of the satellite precisely. [1]

To understand the target response function in more detail the far-field diffraction pattern (FFDP) needs to be analysed further. Based on the idea of Toshimichi Otsubo (Hitotsubashi University, Japan) an experiment is carried out to determine the FFDP of a few selected satellites at the Geodetic Observatory Wettzell.

This paper focuses on the data preparation for this experiment to allow an organized analysis. Therefore, the experiment is described briefly. The exact setup will not be outpointed as well as results of the experiments are not described here. First, the reasons for carrying out this experiment are outlined. Afterwards the basic structure of the experiment is described. Then the key idea and the structure of the database is explained and the different evaluation parameters are presented.

II. KEY IDEA OF THE EXPERIMENT

A. Motivation for carrying out the experiment

The current challenges of the SLR community can be roughly split into three categories: issues with the timing accuracy of the hardware, the atmosphere ([2]) and the COM correction ([3]).

The main problem of the hardware is that the signal strength affects the delay caused by the detector, known as the time walk effect. This effect causes errors up to a few hundred picoseconds depending on the used detector and signal process

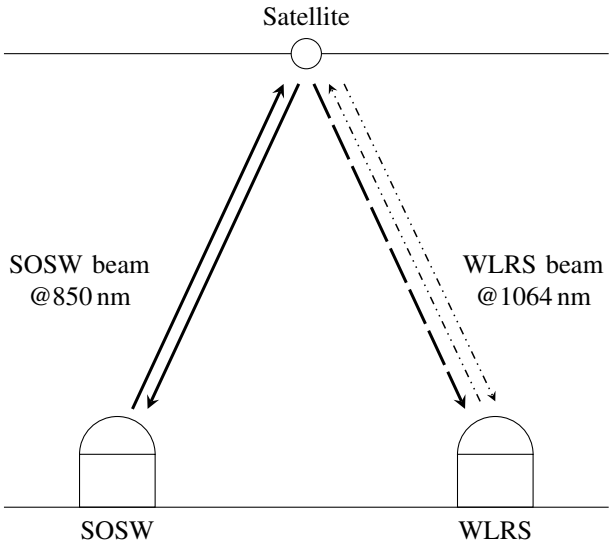

Figure 1. The two SLR systems at the Geodetic Observatory Wettzell are acting in bi-static mode in order to determine the FFDP. The results of the experiment should examine the atmospheric delay and the satellite signature effect.

electronics. There are several ways to solve this issue. On the one hand, the signal strength can be reduced to the single photon level so that the detector is not exposed to signal strength fluctuations. This leads to a loss of some measurement data. Another approach is the use of constant fraction discriminators to reduce range jitter. [4] Also time-walk-compensated Single Photon Avalanche Diodes (C-SPADs) are in use. Those compensate the time walk effect to a few picoseconds. [5] Thus, the error caused by hardware is not believed to be the limiting factor at the moment.

The atmosphere counts to one of the measuring uncertainties. It causes a propagation delay which differs from the delay in vacuum because of the different humidity, temperature and pressure in the atmosphere which in turn cause different refractive indices. In order to estimate the atmospheric delay the local temperature, humidity and pressure are recorded. This method was first introduced by Marini and Murray in 1973 [6]. As this is only a model, it was examined by a new method of handling the atmospheric problem: the two-color-laser ranging [7]. With the two-color-laser ranging the atmospheric delay can be determined experimentally which is expound in [8]. This approach faces one main problem: the used detector must be calibrated accurately. The difficulty lies in the different response time for different wavelengths. [4] Furthermore, besides the atmospheric delay there are small eddies in the atmosphere which cause the twinkling of the light from astronomical objects, also known as scintillation effect. In addition, eddies which cross the whole optical beam lead to a displacement of the whole beam, called the beam wander effect. [9] These effects cannot be predicted by the method of Marini and Murray because those are based on local weather data. Neither can the two-color-laser ranging detect a beam wander effect because there have to be at least two receivers in space.

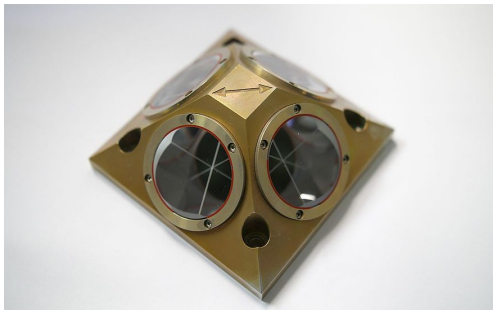

Figure 2. The examined retroreflector was first designed for the CHAMP satellite. The arrow indicates the Nominal flight direction of the satellite. The whole retroreflector is always pointed Nadir. [12]

The next challenging subject is the COM correction. It has been discovered that the COM correction depends on the satellite and the station. The target response function also plays a major role in this topic. It was published by Otsubo and Appleby in 2003 ([1]) that theoretical formulas cannot be validated by measurements adequate enough. They already mention that the FFDP needs to be taken into consideration more closely. [1]

So far, the FFDP of the retroreflectors has been investigated theoretically and experimentally in the laboratory [10]. In addition, some simulated space environments experiments ([11]) yielded results to improve the understanding of the FFDP but no experiment has been performed under real SLR conditions. Real SLR conditions consider the unknown atmosphere and also the actual target response function.

B. Concept of the experiment

To conduct the experiment the two SLR systems at the Geodetic Observatory Wettzell, the Satellite Observing System Wettzell (SOSW) and the Wettzell Laser Ranging System (WLRS), are acting in bi-static mode as can be seen in Fig. 1. This means both of them are observing the same satellite. As the SOSW is emitting at a wavelength of 850 nm an additional detector (SAP500-T8) was implemented in the WLRS receiving unit. This allows the detection of the SOSW signal at the position of the SOSW and the WLRS. Thus, two receivers are realized. The WLRS is also observing the same satellite at a wavelength of 1064 nm. If the 1064 nm detector of the WLRS receives a signal, it can be ensured that the satellite is in the field of view of the WLRS.

As a result, the FFDP can be determined. This results in the constellation already shown in Fig 1. The SOSW and WLRS are about 60 m apart of each other. Due to the small distance between the two SLR systems only the FFDP of low earth orbit satellites at an altitude of about 500 km can be resolved. Furthermore, only satellites equipped with the retroreflector first designed for the CHAMP satellite will be analyzed. Fig. 2 shows the retroreflector. It consists of only 4 reflectors. The arrow on the front face indicates the

direction of the movement of the satellite. The front face where the arrow is imprinted is always oriented towards Nadir which means to the geocenter. Hence, this special retroreflector has two basic advantages over others: first, as it is always pointed Nadir and the velocity vector is known the orientation of the individual reflector is given at any moment and second, it only exists of four retroreflectors, so that one can determinate the illuminated reflector and its orientation. In summary, the following satellites will be observed: SWARM A, SWARM B, SWARM C, TanDEM-X, TerraSAR-X, GRACE-FO 1, GRACE-FO 2, PAZ and KOMPSAT-5.

III. Implemented Data Base

A. Key idea of the data base

To organize the data provided by the two SLR systems a data base is implemented and tables are created. The data base should allow to filter the data and derive the FFDP under different conditions. These conditions are made up by a few evaluation criteria which influence the FFDP. If the data is analyzed it should be possible to define ranges of values for the individual evaluation criteria. The design of the data base is outlined in Fig. 3. Four tables were created. The provided data is split in the WLRS data of the 1064 nm (sat_npt_statistics_WLRS_1064) and the 850 nm detector (sat_npt_statistics_WLRS_850) as well as the SOSW data of the 850 nm detector (sat_npt_statistics_SOSW_850). Furthermore, a table with astronomical seeing predictions was established (dat_pred_seeing). Each table with detector data provides the basic passage information which will be described in chapter III-B. The SOSW 850 nm data table will contain further information which is needed to determine the FFDP. In addition, a primary key is defined for each table to assign the data of each table later. For this purpose, the date (epoch_date) and the time in seconds of the day (SOD) (epoch_SOD) is selected.

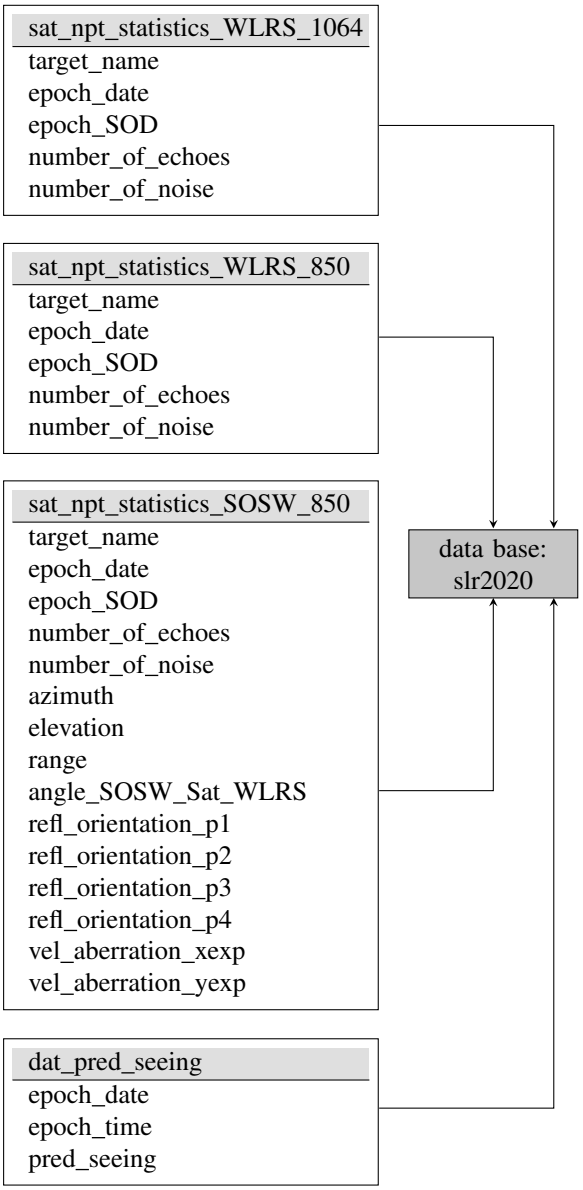

Figure 3. The structure of the data base should allow a organized analysis of the collected data. It consists of the four tables and the parameters shown.

B. Basic passage information

The basic passage information consists of the target name (target_name), the date (epoch_date), the time in SOD (epoch_SOD), the number of echo events (number_of_echoes) and the the number of noise events (number_of_noise). These five values are saved in each table that contains detector information. In addition, elevation, azimuth and the range of the satellite with respect to the SOSW are added to the SOSW table. As well as the angle between the SOSW, satellite and WLRS (angle_SOSW_Sat_WLRS) to plot the FFDP depending on this angle.

C. Astronomical seeing

An extra table for the astronomical seeing prediction is created which also contains the primary key of date and SOD. The astronomical seeing is basically known as a parameter that holds an estimation of the amount of the apparent blurring and twinkling of astronomical objects. Therefore, it may contain a reference to current beam wander and scintillation. To get an estimation of the current astronomical seeing prediction data of the weather forecast provider meteoblue is downloaded. The prediction data is given in arcsec and in a one hour resolution. It might need to be analyzed if the prediction data is adequate enough. Despite that, this parameter should give a rough estimation about the current atmospherically behavior.

D. Orientation of the reflector

If the retroreflector of the satellite is tilted, the effective area of the retroreflector and therefore also the cross section decreases. The diameter of the FFDP will increase. [13] To allow an evaluation of this parameter the orientation of each of the four retroreflectors on board of the chosen satellites is calculated. As only the diameter of the FFDP parallel to the

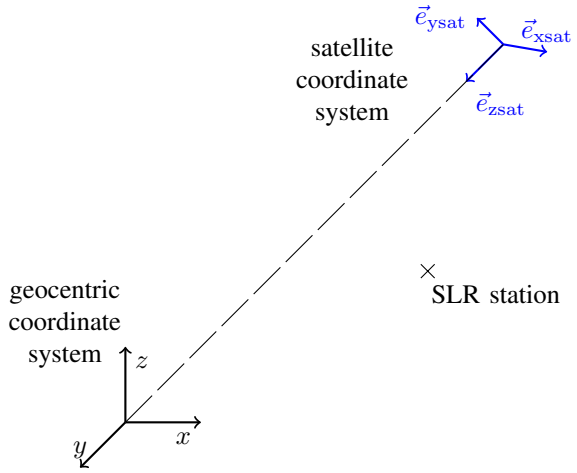

Figure 4. The satellite coordinate system visualized in the geocentric coordinate system which is clearly identified by its origin $\vec{p}_{\mathrm{sat}}$ and its unit vectors ($\vec{e}_{\mathrm{xsat}}$, $\vec{e}_{\mathrm{ysat}}$, $\vec{e}_{\mathrm{zsat}}$).

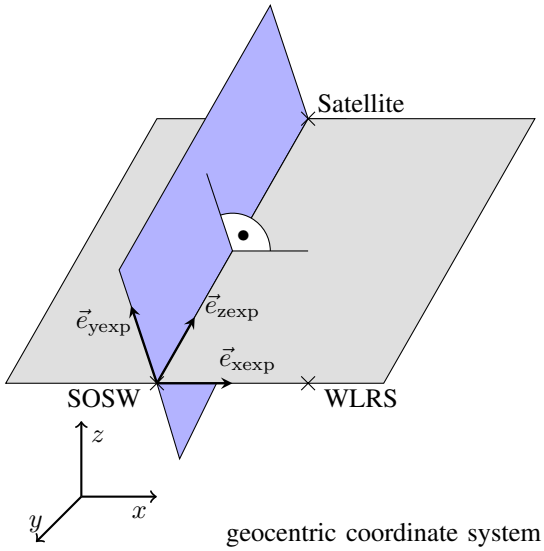

Figure 5. The experimental coordinate system is set up to determine the FFDP in space. It is illustrated by the XZ- (in gray) and YZ-planes (in blue) here.

SOSW and WLRS is of interest, because only a signal in this line of sight can be detected, a projection is performed. The calculation is now demonstrated in detail.

Three different coordinate systems are used:

1) Geocentric coordinate system:
Known as the ECEF (earth-centered, earth-fixed) coordinate system
   - Origin: COM of the earth
   - X-axis: intersects with the Greenwich mean meridian
   - Y-axis: orthogonal to X- and Z-axis
   - Z-axis: rotation axis of the earth

   [14]
2) Satellite coordinate system:
The satellite coordinate system is embedded in the geocentric coordinate system as shown in Fig. 4.
   - Origin: COM of the satellite (it is sufficient to suggest that the COM is equal to location of the reference point of the retroreflector array)
   - X-axis: Nominal flight direction
   - Y-axis: Forming a right handed system with the X- and Z-axis
   - Z-axis: Nominal Nadir direction (vector pointing from satellite to geocenter)
3) Experimental coordinate system:
For the calculation of the FFDP a new coordinate system had to be defined. It is visualized in Fig. 5 with respect to the geocentric coordinate system.
   - Origin: SOSW
   - Y-axis:

$$\vec{e}_{\mathrm{yexp}} = (\vec{p}_{\mathrm{SOSW}} - \vec{p}_{\mathrm{WLRS}}) \otimes (\vec{p}_{\mathrm{sat}} - \vec{p}_{\mathrm{SOSW}}) \quad (1)$$

   - X-axis:

$$\vec{e}_{\mathrm{xexp}} = (\vec{p}_{\mathrm{sat}} - \vec{p}_{\mathrm{SOSW}}) \otimes \vec{e}_{\mathrm{yexp}} \quad (2)$$

   - Z-axis: vector from SOSW to satellite

Provided parameters:

1) Orientation of the normal vectors of the retro faces in the satellite coordinate system $\vec{n}_{\mathrm{r},i\_\mathrm{sat}}$ with ($i = 1,\ 2,\ 3,\ 4$): number of the retroreflector (given in [15], visualized in Fig. 6)
2) Position ($\vec{p}_{\mathrm{sat}}$) and velocity vector ($\vec{v}_{\mathrm{sat}}$) of the satellite in the geocentric coordinate system
3) Coordinates of the two SLR stations, SOSW $\vec{p}_{\mathrm{SOSW}}$ and WLRS $\vec{p}_{\mathrm{WLRS}}$, in the geocentric coordinate system

Calculation:

1) Determination of the transformation matrix for the conversion of the satellite coordinate system to the geocentric coordinate system:
The satellite coordinate system is characterized by its origin ($\vec{p}_{\mathrm{sat}}$) and the three unit vectors ($\vec{e}_{\mathrm{xsat}}, \vec{e}_{\mathrm{ysat}}, \vec{e}_{\mathrm{zsat}}$) in the geocentric coordinate system, see Fig. 4. The unit vectors can be derived as follows:

$$\begin{aligned} \vec{e}_{\mathrm{xsat}} &= \frac{\vec{v}_{\mathrm{sat}}}{|\ \vec{v}_{\mathrm{sat}}\ |} \\ \vec{e}_{\mathrm{zsat}} = \vec{e}_{\mathrm{nadir}} &= \frac{-\vec{p}_{\mathrm{sat}}}{|\ \vec{p}_{\mathrm{sat}}\ |} \\ \vec{e}_{\mathrm{ysat}} &= \vec{e}_{\mathrm{xsat}} \otimes \vec{e}_{\mathrm{zsat}} \end{aligned} \quad (3)$$

For the transformation matrix, the coordinate vectors are arranged next to each other in column notation.

$$\boldsymbol{M}_{\mathbf{Sat \rightarrow Geo}} = \begin{bmatrix} e_{\mathrm{xsat_x}} & e_{\mathrm{ysat_x}} & e_{\mathrm{zsat_x}} \\ e_{\mathrm{xsat_y}} & e_{\mathrm{ysat_y}} & e_{\mathrm{zsat_y}} \\ e_{\mathrm{xsat_z}} & e_{\mathrm{ysat_z}} & e_{\mathrm{zsat_z}} \end{bmatrix} \quad (4)$$

2) Transformation of the normal vectors of the retroreflector faces into the geocentric coordinate system:
The normal vectors of the reflectors $\vec{n}_{\mathrm{r},i\_\mathrm{sat}}$ shall be

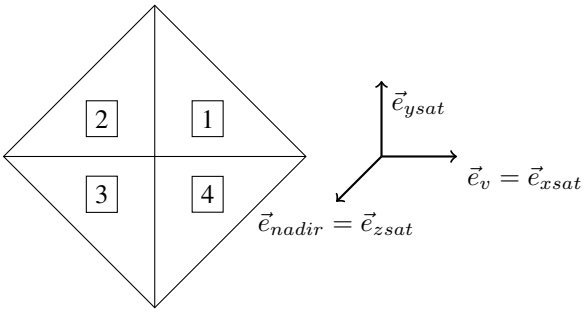

Figure 6. The retroreflector array is arranged in a pyramid-like pattern. The Nominal flight and the Nadir direction are establishing the satellite coordinate system.

described in the geocentric coordinate system. A normal vector of a plane must be transformed with transposed inverse of the transformation matrix.

$$\vec{n}_{\mathrm{r},i\_\mathrm{geo}} = (\boldsymbol{M}_{\mathbf{Sat\rightarrow Geo}}{}^{-1})^T \cdot \vec{n}_{\mathrm{r},i\_\mathrm{sat}} \tag{5}$$

3) Setting the XZ-plane of the experiment coordinate system:

$$\vec{n}_{\mathrm{xzexp}} = \vec{e}_{\mathrm{yexp}} \tag{6}$$

4) Projection of the normal vectors of the retro faces (in geocentric coordinate system) into the XZ-plane of the experiment coordinate system:
The projection of $\vec{n}_{\mathrm{r},i\_\mathrm{geo}}$ onto the XZ-plane of the experimental coordinate system can be calculated by subtracting the orthogonal component of $\vec{n}_{\mathrm{r},i\_\mathrm{geo}}$ from the respective plane.

$$\begin{aligned} \vec{n}_{\mathrm{r},i\_\mathrm{xzexp}} &= \vec{n}_{\mathrm{r},i\_\mathrm{geo}} - \vec{n}_{\mathrm{r},i\_\perp\mathrm{xzexp}} \\ \vec{n}_{r,i\_\perp\mathrm{xzexp}} &= \frac{\vec{n}_{\mathrm{r},i\_\mathrm{geo}} \cdot \vec{n}_{\mathrm{exp}}}{\mid \vec{n}_{\mathrm{xzexp}} \mid^2} \cdot \vec{n}_{\mathrm{xzexp}} \end{aligned} \tag{7}$$

5) Calculation of the tilt angle seen from the SOSW and WLRS:
The angle $\gamma_{\parallel}$ is the angle between $\vec{n}_{\mathrm{r},i\_\mathrm{xzexp}}$ and the line of sight from SOSW to satellite.

$$\vec{p}_{\mathrm{sat2SOSW}} = \vec{p}_{\mathrm{SOSW}} - \vec{p}_{\mathrm{sat}} \tag{8}$$

$$\gamma_{\parallel,i} = \arccos\left(\frac{\vec{n}_{\mathrm{r},i\_\mathrm{xzexp}} \cdot \vec{p}_{\mathrm{sat2SOSW}}}{\mid \vec{n}_{\mathrm{r},i\_\mathrm{xzexp}} \mid \cdot \mid \vec{p}_{\mathrm{sat2SOSW}} \mid}\right) \tag{9}$$

I.e. when $\gamma_{\parallel,i}$ accounts 0° the reflector i is illuminated vertically. The angle $\gamma_{\parallel,1}$ is saved as refl_orientation_p1. The same format applies for the other angles $\gamma_{\parallel,i}$.

E. Velocity aberration

A relative velocity between satellite and station causes the reflected beam to be shifted by the angle α_{geo} in the direction of the velocity vector $\vec{v}_{\mathrm{sat}}$ [13]. The effect is visualized in Fig. 7.

$$\vec{\alpha}_{geo} = \frac{2\vec{v}_{\mathrm{sat}}}{\mathrm{c}} \tag{10}$$

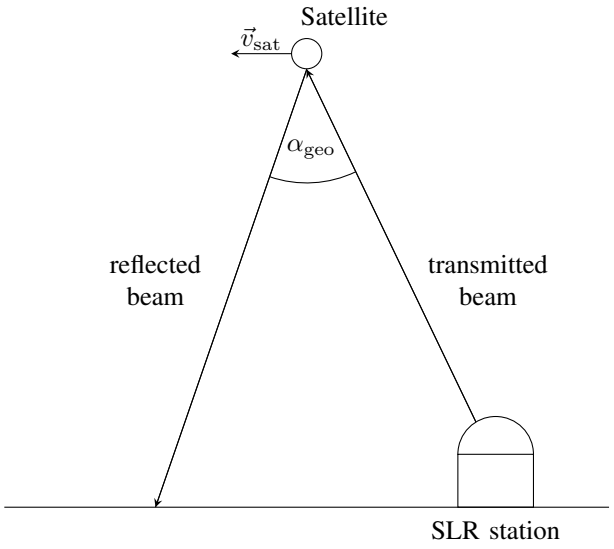

Figure 7. The effect of velocity aberration: a relative velocity between satellite and station causes the reflected beam to be shifted by the angle α_{geo}.

To relate the effect of velocity aberration to the experimental coordinate system described in chapter III-D, $\vec{\alpha}_{\mathrm{geo}}$ is projected on the X- and Y-axis of the experimental coordinate system:

$$\begin{aligned} \vec{\alpha}_{\mathrm{xexp}} &= \frac{\vec{e}_{\mathrm{xexp}} \cdot \vec{\alpha}_{\mathrm{geo}}}{\mid \vec{e}_{\mathrm{xexp}} \mid^2} \cdot \vec{e}_{\mathrm{xexp}} \\ \vec{\alpha}_{\mathrm{yexp}} &= \frac{\vec{e}_{\mathrm{yexp}} \cdot \vec{\alpha}_{\mathrm{geo}}}{\mid \vec{e}_{\mathrm{yexp}} \mid^2} \cdot \vec{e}_{\mathrm{yexp}} \end{aligned} \tag{11}$$

The final value of the velocity aberration on the respective axis is the amount of $\vec{\alpha}_{\mathrm{xexp}}$ and $\vec{\alpha}_{\mathrm{yexp}}$. The direction of the displacement on the X- or Y-axis is determined by the linear dependence of $\vec{\alpha}_{\mathrm{xexp}}$ or $\vec{\alpha}_{\mathrm{yexp}}$ and the respective axis.

F. Temperature of the reflector

Tests of the reflector in simulated space environment showed the dependency of the FFDP and sun exposure. After one hour heating with a sun simulator the FFDP is expanded and it is relaxed to its usual size after 10 minutes of no heating. [11] As the information about the temperature of the reflector is not available and changes only occur during sunlight exposure and 10 minutes afterwards, no data is recorded at the moment. Nonetheless, it would be possible to determine whether the reflector is currently exposed to sunlight or not if it is needed in the analysis.

IV. Exemplary Outcome of the Data Preparation

In order to illustrate the processing of the data, a sample calculation is presented. The used data is from the satellite SWARM B of the 2020-03-24. Furthermore, the parameters in Table I are provided.

Table II shows the calculated evaluation criteria according to chapter III. Notice that the satellite was high on the horizon at this point in time because of an elevation of 63°. The reflector 1 and 4 are not accessible in this configuration because they

Table I
PROVIDED PARAMETERS

	X	Y	Z
$\vec{p}_{\mathrm{WLRS}}$	4075576.8 m	931785.5 m	4801583.6 m
$\vec{p}_{\mathrm{SOSW}}$	4075531.073 m	931781.841 m	4801619.951 m
$\vec{p}_{\mathrm{sat}}$	4356459.713 m	1252853.163 m	5165529.756 m
$\vec{v}_{\mathrm{sat}}$	5464.34 m/s	1699.69 m/s	-5007.72 m/s

Table II
CALCULATED EVALUATION CRITERIA

azimuth	6°
elevation	63°
range	560746.88 m
angle_SOSW_Sat_WLRS	1.90 arcsec
refl_orientation_p1	72°
refl_orientation_p2	8°
refl_orientation_p3	6°
refl_orientation_p4	85°
vel_aberration_xexp	8.0 arcsec
vel_aberration_yexp	1.0 arcsec

are tilted above the cut-off angle of the reflectors of about 43° while the reflectors 2 and 3 have an influence on the FFDP with respect to the SOSW-WLRS line of sight. One can determine the theoretic displacement of the FFDP through the velocity aberration. In this case, the FFDP is displaced by 8 arcsec in direction of the WLRS.

V. DISCUSSION

The database allows an organized evaluation of the collected data. It is possible to analyze the influence of the atmosphere and reflector orientation on the FFDP. The various criteria were selected on the basis of previous research. Only one criterion, the temperature of the reflector, was found to be a FFDP modifying feature, but was not included in the database. This is because there is no information available. Should the analysis require the specification of this feature, it could be determined whether the reflector was illuminated by the sun or not.

VI. OUTLOOK

To analyze the FFDP the experiment has to be carried out and the data has to be added to the data base. As many measurement data as possible must be collected under different conditions. Afterwards, the structure of the FFDP can be determined in a real and non-simulated SLR environment. If the experiment is continued e.g. by observing other satellites with different reflectors, the difference between the reflectors could possibly be made clear. Collecting information about the FFDP can help to understand the target response function. Furthermore, this will be the first experiment that examines two different SLR stations with almost similar atmospheric conditions. Thus, the outcome of the experiment will also be interesting in this respect.

ACKNOWLEDGMENT

The authors would like to thank Stefan Marz (Technische Universität München, Munich) for first suggestions with regard to the calculation of the reflector orientation and of course Toshimichi Otsubo (Hitotsubashi University, Japan) for the idea of the experiment.

REFERENCES

[1] T. Otsubo and G. M. Appleby, "System-dependent center-of-mass correction for spherical geodetic satellites," *Journal of Geophysical Research: Solid Earth*, vol. 108, no. B4, 2003.

[2] J. Degnan, "Millimeter Accuracy Satellite Laser Ranging: A Review," in *Contributions of Space Geodesy to Geodynamics: Technology*, vol. 25, pp. 133–162, Jan. 1993.

[3] T. Otsubo, R. A. Sherwood, G. M. Appleby, and R. Neubert, "Center-of-mass corrections for sub-cm-precision laser-ranging targets: Starlette, Stella and LARES," *Journal of Geodesy*, vol. 89, pp. 303–312, Apr. 2015.

[4] M. Wilkinson, U. Schreiber, I. Procházka, C. Moore, J. Degnan, G. Kirchner, Z. Zhongping, P. Dunn, V. Shargorodskiy, M. Sadovnikov, C. Courde, and H. Kunimori, "The next generation of satellite laser ranging systems," *Journal of Geodesy*, vol. 93, pp. 2227–2247, Nov. 2019.

[5] G. Kirchner, F. Koidl, J. Blazej, K. Hamal, and I. Prochazka, "Time-walk-compensated SPAD: multiple-photon versus single-photon operation," in *Laser Radar Ranging and Atmospheric Lidar Techniques*, vol. 3218, pp. 106–112, International Society for Optics and Photonics, Dec. 1997.

[6] J. W. M. Marini, "Correction of laser range tracking data for atmospheric refraction at elevations above 10 degrees," tech. rep., Nov. 1973.

[7] S. Riepl, "Experimental Verification of the MARINI-MURRAY Model by Two Colour SLR," Feb. 2001.

[8] J. B. Abshire and C. S. Gardner, "Atmospheric Refractivity Corrections in Satellite Laser Ranging," *IEEE Transactions on Geoscience and Remote Sensing*, vol. GE-23, pp. 414–425, July 1985.

[9] F. Dios, J. A. Rubio, A. Rodríguez, and A. Comerón, "Scintillation and beam-wander analysis in an optical ground station-satellite uplink," *Applied Optics*, vol. 43, pp. 3866–3873, July 2004.

[10] R. Neubert, L. Grunwaldt, and J. Neubert, "The retro-reflector for the CHAMP satellite: Final design and realization," in *Proceedings of the 11th international workshop on laser ranging*, pp. 260–270, Sept. 1998.

[11] C. Paris and R. Neubert, "Tests of LARES and CHAMP cube corner reflectors in simulated space environment," in *2015 IEEE Aerospace Conference*, pp. 1–9, Mar. 2015. ISSN: 1095-323X.

[12] S. Bauer, "Laser Reflectors for LEO Satellites."

[13] O. Minott, "DESIGN OF RETRODIRECTOR ARRAYS FOR LASER RANGING OF SATELLITES," p. 21, Mar. 1974.

[14] C. Boucher and Z. Altamimi, "ITRS, PZ-90 and WGS 84: current realizations and the related transformation parameters," *Journal of Geodesy*, vol. 75, pp. 613–619, Nov. 2001.

[15] R. Neubert, "The Center of Mass Correction (CoM) for Laser Ranging Data of the CHAMP Reflector," *Issue c 14*, Oct. 2009.